Single chain polymeric nanoparticles to promote selective hydroxylation reactions of phenol catalyzed by copper

Srinivas Thanneeru, a Searle S. Duay, Lei Jin, Youjun Fu, Alfredo Angeles-Boza, Jie He a,b,*

^a Department of Chemistry, and ^b Institute of Materials Science, University of Connecticut, Storrs, CT 06269

ABSTRACT: Metal-containing single chain polymeric nanoparticles (SCPNs) can be used as synthetic mimics of metalloenzymes to catalyze analogous biological reactions. However, the role of folded polymer backbones on the reaction activity and selectivity of metal sites is currently not clear. This communication reports our findings on how polymeric frameworks modulate the coordination of Cu sites and the catalytic activity/selectivity of Cu sites using Cu-containing SCPNs as artificial enzyme mimics for monophenol hydroxylation reactions. Imidazole-functionalized copolymers of poly(methyl methacrylate-*co*-3-imidazolyl-2-hydroxy propyl methacrylate) were used for intramolecular Cu-imidazole binding that triggered the self-folding of polymers simultaneously. Polymer chains were found to impose steric hindrance which limited the Cu-imidazole complexation, to yield unsaturated Cu sites with an average coordination number of 3.3. Cu-containing SCPNs showed a high selectivity for the hydroxylation reaction of phenol, >80%, with a turnover frequency of >870 h⁻¹. We demonstrated that the selectivity to yield catechol was largely influenced by the flexibility of the folded polymer backbone where a more flexible polymer backbone allows the cooperative catalysis of two Cu sites. The second coordination sphere provided by the folded polymer that has been less studied is therefore critical in the design of active mimics of metalloenzymes.

Copper (Cu) plays a key role in many biological redox reactions in nature. ¹⁻⁵ Several metalloenzymes, including galactose oxidase and tyrosinase, have Cu ion(s) as cofactors. For example, tyrosinase, widely distributed in plants, animals and fungi, can catalyze the regioselective hydroxylation of monophenols to catechol derivatives as the first step of melanin synthesis. ⁶ The active site of tyrosinases consists of two adjacent Cu⁺ ions switching between the +2 and +1 oxidation states, ⁷ coordinated by histidine residues, known as "type-3" Cu-sites. ⁵, ⁸, ⁹ Much effort has been made to design Cu-containing complexes that mimic the active sites of tyrosinase and catalyze analogous redox reactions. In the absence of protein frameworks, Cu-containing complexes, however, are not efficient for oxygen activation and catalysis. ¹⁰⁻¹²

Incorporating metal ions into discrete self-folded polymer chains offers a facile way to preparing synthetic mimics of metalloenzymes. 13-24 Folded polymeric frameworks having rich functionalities, controllable hydrophobicity/hydrophilicity and chain flexibility are excellent alternatives to replace (or mimic) protein frameworks of metalloenzymes to some extent. Selffolding is an intramolecular coil-to-particle transition of individual chains that is usually triggered by intramolecular crosslinking at very dilute concentrations. 25-34 The self-folding of polymers can produce ultrasmall, well-defined single chain polymeric nanoparticles (SCPNs) in the range of 2-20 nm, close to the size of metalloenzymes. Since self-folding is usually performed in a good solvent, SCPNs are expected to be loosely collapsed in their swollen state, unlike the folding of natural proteins.³⁵⁻³⁹ This ensures the accessibility of SCPNs to any small molecular substrates. When integrating Cu complexes within SCPNs, the second coordination sphere provided by the folded polymeric frameworks is expected to promote the catalytic activity of metal ions. 40, 41 In the current contribution, we design Cu-containing SCPNs as artificial enzymes for hydroxylation reactions of monophenols. Our synthetic strategy is to use the coordination of copper ions to imidazole ligands to drive

the self-folding of discrete polymer chains of an imidazole-functionalized copolymer of poly(methyl methacrylate-*co*-3-imidazolyl-2-hydroxy propyl methacrylate) (P(MMA-*co*-IHPMA)). Hydroxyl groups that facilitate the movement of protons are part of the second coordination sphere of the metal ion. The Cu-imidazole coordination is used to efficiently and reversibly fold P(MMA-*co*-IHPMA) as confirmed by size-exclusion chromatography (SEC) and NMR spectroscopy. The Cu-containing SCPNs show a selectivity for the hydroxylation reaction of phenol, >80% with a turnover frequency (TOF) of >870 h⁻¹. We demonstrate that the selectivity toward the hydroxylation reaction is largely influenced by the dynamics of folded polymer backbone, known to be critical for the activity of enzymes as well. 42-44

Imidazole-functionalized copolymers of P(MMA-co-IHPMA) were prepared via post-polymerization functionalization (Figure 1a). The parent copolymers of poly(methyl methacrylate-co-glycidyl methacrylate) P(MMA-co-GMA) were synthesized via reversible addition-fragmentation chain transfer polymerization. Post-polymerization functionalization of the parent copolymers was carried out via ring opening reaction of epoxides with excess imidazole (i.e. 10 fold excess with respect to epoxides) in dimethyl sulfoxide (DMSO) at 80 °C to yield P(MMA-co-IHPMA) copolymers. 45-48 The post-polymerization functionalization was confirmed by ¹H NMR spectroscopy and SEC. Using P(MMA₂₁₈-co-GMA₄₃) as an example, the disappearance of diastereotopic proton peaks of methylene groups from GMA units at 4.3, 3.8 ppm and 2.8, 2.7 ppm suggested the occurrence of the ring opening reaction (see Figure 1b). In addition, new peaks at 6.9, 7.1, and 7.6 ppm corresponding to protons on the imidazole ring confirmed the introduction of imidazole moieties. The grafting ratio was estimated to be ca. 100%, to yield P(MMA₂₁₈-co-IHPMA₄₃) (denoted as P1). SEC measurements showed an increase in the number-average molecular weight (M_n) of the copolymer from 56.5 to 128.4 kg/mol with a

dispersity (M_w/M_n) of 1.28 (Figure 1c). There is a small shoulder at a shorter elution time that may be due to the interchain cross-coupling in the ring opening reaction and/or weak absorption of imidazole to SEC columns.^{48, 49} Another copolymer with

a higher content of imidazole P(MMA₂₇₃-co-IHPMA₁₃₄) (P2) was also prepared to examine the effect of the imidazole content on the self-folding (see Table 1 and Figure S1).

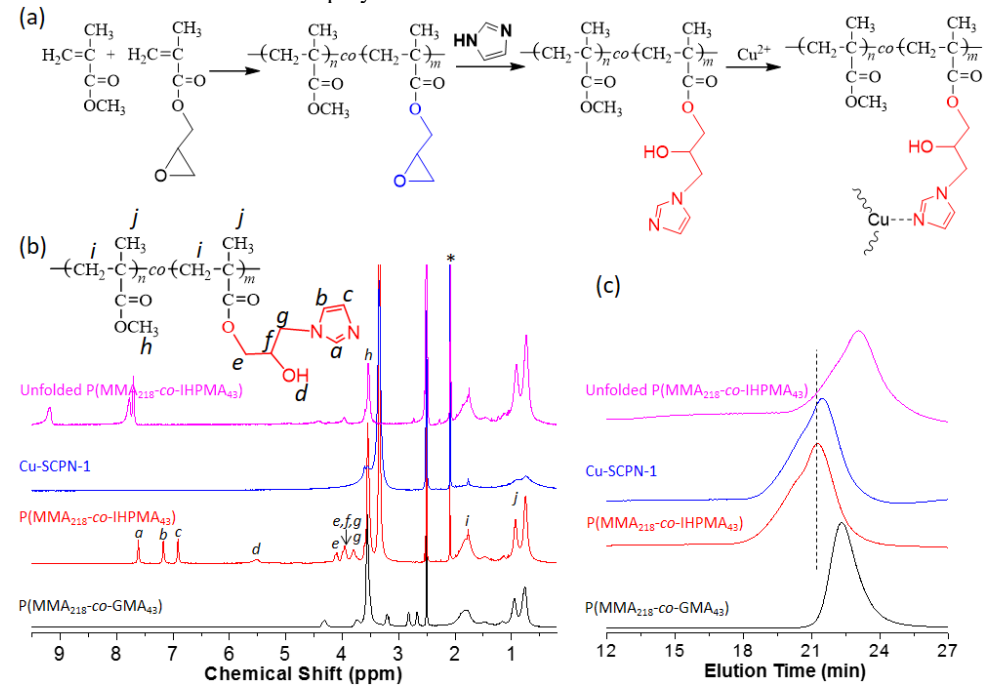


Figure 1. (a) Synthetic routes to preparing imidazole-functionalized copolymers. (b,c) 1 H NMR spectra and SEC elution curves of P(MMA₂₁₈-co-GMA₄₃) (black), P(MMA₂₁₈-co-IHPMA₄₃) (red), its Cu-SCPN F1 (blue) and unfolded P1 (pink). All NMR spectra were collected in d_6 -DMSO and the SEC measurements were performed in DMAc. The peak * is from acetone.

Cu-SCPNs were prepared by utilizing the intramolecular Cu-imidazole coordination that triggers the self-folding of individual polymer chains simultaneously. The intramolecular Cuimidazole coordination was carried out in a good solvent for the linear copolymers, such as N,N'-dimethylformamide (DMF) or N,N'-dimethylacetamide (DMAc). The coil-to-particle transition of discrete polymer chains results in the formation of Cu-SCPNs where the folded polymer backbone as a whole serves as the second coordination environment for the incorporated Cu sites. The Cu-imidazole coordination was examined using ¹H NMR spectroscopy (Figure 1b). In a good solvent for the linear copolymer of P1 (d_6 -DMSO), all protons of MMA and imidazole units were indicated in the solution. After adding Cu(NO₃)₂ as a Cu source, the resonance feature of polymer side chains completely disappeared. The peaks of methylene (i, Figure 1b) and methyl (j, Figure 1b) groups on the backbone showed obvious broadening. This is attributed to the loss of the chain mobility of polymer and the presence of paramagnetic Cu²⁺ ions.

Self-folding of the copolymers was evidenced by SEC measurements. For P1, the M_n decreased from 128.4 kg/mol to 114.0 kg/mol along with a small increase in its elution time (Figure 1c), corresponding to the shrinkage of hydrodynamic volume ~11.5 %. The volume shrinkage is small in terms of the decrease in molecular weight; but it is in good agreement with other reports on intramolecular cross-linking of polymers via non-covalent interactions.^{19, 22, 37, 50} A recent report from Pomposo *et al.* shows that the expected size (*R*) of polymer upon intrachain folding via reversible non-covalent cross-linking is given by.³⁷

$$R = R_0 (1 - x)^{0.6}$$

where x is the fraction of cross-linkable functional groups in polymer chain involved in reversible bonds, and R and R_0 are

the expected size of folded polymer and the size of linear polymer, respectively. The expected size of the folded polymer (R)should be $R = 0.9 \times R_0$ for P1. Given $R \propto M^{0.588}$, 51 the expected shrinkage in molecular weight is 16.4% for P(MMA218-co-IHPMA₄₃), fairly close to our observed value from SEC. It should be noted that, the magnitude of the decrease in M_n for copolymer P2 is smaller when compared to that of copolymer P1 after Cu-imidazole complexation. This can be attributed to the increase in number of imidazole moieties in P2 leading to strong interactions with the SEC columns (note that, P2 and its SCPNs cannot be eluted in DMAc in the absence of LiCl).⁴⁹ The absence of peaks at a shorter elution time suggested the Cu-imidazole coordination occurred intramolecularly to drive the selffolding of discrete polymer chains that reduced the hydrodynamic volume of chains. The Cu-to-imidazole ratio seems to have a minimum influence on the change of the apparent molecular weight of the final Cu-SCPNs. No further decrease in molecular weight of Cu-SCPNs was seen when the Cu-to-imidazole ratio reached to 0.25 (Figure S2). The change in hydrodynamic diameters was confirmed by dynamic light scattering (DLS). The linear copolymer of P(MMA₂₁₈-co-IHPMA₄₃) has a hydrodynamic radius of 5.8 nm in DMAc, while its Cu-SCPNs reduced to 3.7 nm (Figure S3). These findings confirmed the intramolecular folding of the linear copolymers upon Cu-imidazole coordination.

To confirm whether the folding was triggered by Cu-imidazole complexation, the dissociation of Cu-imidazole complex of Cu-SCPNs was further investigated by adding HCl solution using ¹H NMR spectroscopy. The quaternization of imidazole with the addition of HCl solution (10 equivalences relative to imidazole) can disrupt Cu-imidazole complexation. This is evidenced by the reappearance of all resonance peaks of the linear copolymer as exhibited in Figure 1b. The dissociation of Cuimidazole complexes thus led to the unfolding of the copolymers, since the NMR peaks of methyl and methylene groups of PMMA became prominent. A downfield shift of proton peaks on the imidazole ring (8-10 ppm) occurred as a result of the protonation of imidazole. The unfolded P1 was also examined by SEC, in which an increase in elution time, compared to its linear copolymer, was observed (Figure 1c), likely due to the interaction of the positively charged copolymer with SEC columns. ⁵²

Table 1. Molecular weights and hydrodynamic diameters of the two linear copolymers and their SCPNs

Polymers ^a	$M_{ m n, NMR}$ (kg/mol) a	$M_{ m n,SEC}$ (kg/mol) b	\mathbf{H} $(\mathbf{M}_{\mathbf{w}}/\mathbf{M}_{\mathbf{n}})^b$	R_h (nm) c
P(MMA ₂₁₈ -co-GMA ₄₃)	27.9	56.5	1.19	
P(MMA ₂₁₈ -co- IHPMA ₄₃)	30.6	128.4	1.28	5.8
P(MMA ₂₇₃ -co- GMA ₁₃₄)	46.3	53.8	1.21	
P(MMA ₂₇₃ -co- IHPMA ₁₃₄)	55.2	119.4	1.36	6.1
Cu-SCPN-1 d	-	114.0	1.28	3.7
Cu-SCPN-2 d	-	112.5	1.38	2.6

Note: ^a M_n determined from ¹H NMR; ^b M_n determined from SEC; ^c D_h is the hydrodynamic radius measured using DLS; ^d Cu-SCPN-1 and Cu-SCPN-2 were prepared using the P(MMA₂₁₈-co-IHPMA₄₃) and P(MMA₂₇₃-co-IHPMA₁₃₄) at a Cu-to-imidazole ratio of 1:1 (mol), respectively. ¹H NMR was measured in d_o -DMSO, while both SEC and DLS measurements were performed in DMAc.

The formation of Cu-imidazole complexes was confirmed by UV-vis spectroscopy. To remove the unbound Cu²⁺ ions, asprepared Cu-SCPNs were dialyzed against water for 24 h. Both Cu-SCPNs from P1 and P2 showed a good solubility in water as confirmed by DLS (see Figure S3). The hydrodynamic radius of Cu-SCPN-1 in water was determined to be 11.5 nm. It suggested that Cu-SCPN-1 formed small micelles that were stabilized by hydrophilic imidazole and hydroxyl groups on the SCPN. On the other hand, the hydrodynamic radius of Cu-SCPN-2 in water is found to be only 1.4 nm. It suggested Cu-SCPN-2 formed more compact folding driven by the hydrophobic interaction of the PMMA backbone. The hydrophobicity of polymer backbones is responsible for the inter- or intramolecular collapse of SCPNs when changing the solvent to water.⁵³ The Cu-SCPN-1 from P1 displays two distinct peaks at 278 nm (strong), and 670 nm (weak), attributed to the Cu-imidazole charge-transfer band and d-d transitions of Cu²⁺ ions, respectively.⁵⁴ Upon addition of HCl, the two peaks at 278 nm and 670 nm disappeared, indicating the dissociation of Cu-imidazole complexes.⁵⁵ In contrast, the linear copolymer of P1 shows no obvious absorption in the range of 300-800 nm and a weak absorption peak at 276 nm was assigned to $n\rightarrow\pi^*$ of carbonyl groups. Cu(NO₃)₂ in aqueous solution exhibited a broad, weak feature centered at ~810 nm, due to the Laporte-forbidden d-d transition of [Cu(H₂O)₆]^{2+.56} Similar results were observed for the Cu-SCPN-2 of P1 (Figure S4). Using the absorption of the d-d transition, we estimated the average number of Cu sites per SCPN to be ca. 6.4 for the Cu-SCPN-1 of P1, and 18.7 for the Cu-SCPN-2 of P2. The incorporation of Cu²⁺ ions was further confirmed using electron paramagnetic resonance (EPR) spectroscopy (Figure S5). Since the EPR spin signal is determined by the total number Cu²⁺ ions, the average number of Cu sites per Cu-SCPN-1 of P1 was measured to be ca. 6.8 by averaging the total spin states to the total number of Cu-SCPNs. This value

is in good agreement to that obtained from UV-vis spectroscopy.

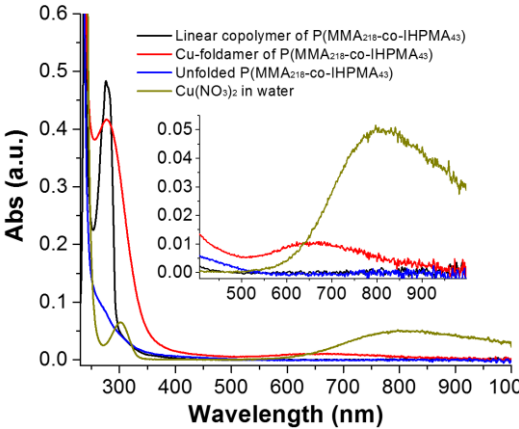


Figure 2. UV-vis spectra of the linear copolymer of P(MMA₂₁₈-co-IHPMA₄₃) (black), the Cu-SCPN of P(MMA₂₁₈-co-IHPMA₄₃) (red), unfolded P(MMA₂₁₈-co-IHPMA₄₃) (blue), and Cu(NO₃)₂ (dark yellow). The UV-vis spectrum of the linear copolymer of P(MMA₂₁₈-co-IHPMA₄₃) was recorded in THF/methanol (5:1, vol); while the other three were measured in water. The concentration of the linear copolymer and Cu(NO₃)₂ is 1mg/mL, and the Cu-SCPN and the unfolded polymer is 0.9 mg/mL

The binding affinity of Cu to the imidazole-functionalized copolymer was measured by titrating the linear copolymer with Cu^{2+} ions. In brief, at a fixed polymer concentration (1 mg/mL) in DMAc, $Cu(NO_3)_2$ was added until no more increase in absorbance at 670 nm was observed, indicating the saturation coordination of Cu-to-imidazole. The fraction of saturation, denoted by θ , was calculated by normalizing the absorbance at 670 nm to the maximum absorbance at saturation point. The fraction of saturation, denoted by θ , is a function of the total concentration of Cu^{2+} ions and the binding constant, K_b , as given in the equation (see SI for the analysis),⁵⁷

$$\theta = \frac{K_b \left[\text{Cu}^{2+} \right]}{1 + K_b \left[\text{Cu}^{2+} \right]}$$

The binding constant K_b can be extracted to be $10^{2.98}$ M⁻¹ for P(MMA₂₁₈-co-IHPMA₄₃) by plotting $1/\theta \ vs. \ 1/[Cu^{2+}]$ (Figure S6). The binding stoichiometry of Cu was estimated from Job's plot by continuously varying the ratios of Cu-to-imidazole (see experimental details in SI). The average coordination number of Cu^{2+} ions in Cu-SCPN-1 was estimated to be ca. 3.3 (Figure S7). Compared to the theoretical coordination number of Cu²⁺ ions (i.e., 4 for a square planar coordination for Cu²⁺), our results suggest that polymer chains impose steric hindrance to limit the number of imidazole ligands coordinated to Cu. The unsaturated Cu sites in turn may favor the binding of reactants in catalysis. Although the binding affinity of Cu to copolymers is low, the SCPNs are stable at higher temperatures. The temperature-dependent ¹HNMR spectra of Cu-SCPN-1 shown in Figure S8 did not indicate any obvious dissociation of SCPNs up to 67 °C.

The catalytic activity of Cu-SCPNs was examined for hydroxylation of phenols using H₂O₂ as an oxidant in water at 60 °C.⁵⁸ The conversion of phenol and the product selectivity was calculated from HPLC-MS and ¹H NMR using DMF as an internal standard (see SI for experimental details). The primary products obtained were identified as catechol (CAT) and hydroquinone (HQ). A trace amount of benzoquinone (BQ), <0.5%,

was detected from HPLC-MS (Figures S9-11). The catalytic activity of Cu-SCPN-1 of P(MMA $_{218}$ -co-IHPMA $_{43}$) was first carried out in excess of phenol (3160-fold relative to that of Cu sites) at different concentrations of H_2O_2 . The selectivity of CAT and HQ and the conversion of phenol results were summarized in Table 2. At an optimal ratio of phenol to H_2O_2 (1:2, mol), a high selectivity of 85.1% toward the 1,2-hydroxylation (CAT) was obtained.

Cu-SCPN-1 and Cu-SCPN-2 were carefully examined to study the influence of Cu loading on the reaction kinetics and selectivity as given in Figure 3. Both SCPNs show very similar activity where >50% conversion of phenol was achieved at 1.5 h. Given that the copper loading in Cu-SCPN-2 is significantly higher than that in Cu-SCPN-1, it suggests that the collapse degree of polymer chains has very limit impact on the accessibility of Cu sites. However, Cu-SCPN-1 shows a higher selectivity towards CAT throughout, compared to Cu-SCPN-2. The selectivity to catechol varied in the range of 96%-73% using Cu-SCPN-1; while, only 78%-54% using Cu-SCPN-2. This is likely caused by the difference in the flexibility of folded polymer chains of Cu-SCPN-1 and Cu-SCPN-2. The flexibility of polymer chain will be largely limited in the presence of Cu-imidazole complexes. Since Cu-SCPN-2 has a higher content of Cu ions, the SCPN becomes less flexible. It has been known that, the hydroxylation of phenol is achieved cooperatively by

two Cu sites. Only when the two Cu²⁺ ions are close in the distance of 3-5 Å, they can bind to phenol and transfer the oxygen to the *ortho* position to generate CAT.^{5, 59, 60} In the case of Cu-SCPN-2, the stiffness of the polymer chains possibly limits the dynamic properties of adjacent Cu ions to co-catalyze the hydroxylation. Therefore, the folded polymer chains can tune the conformational landscape to modulate the reaction selectivity.

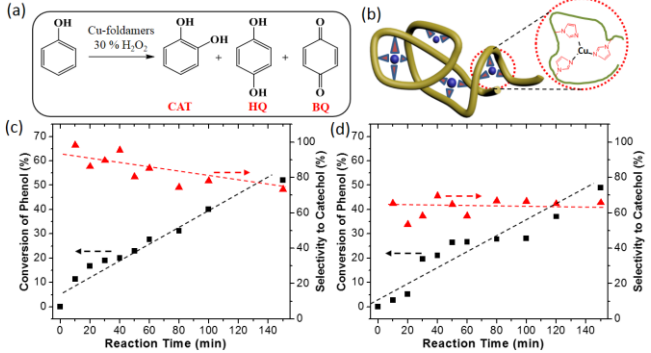


Figure 3. (a) Schematics of phenol hydroxylation reaction catalyzed by Cu-SCPNs. (b) Schematic illustration of Cu-imidazole complexes in SCPNs (a coordination number of 3). (c,d) Kinetic plots of phenol hydroxylation catalyzed by Cu-SCPN-1 (c) and Cu-SCPN-2(d). Reaction conditions in c and d: Cu/phenol/ $H_2O_2 = 1/3160/6320$ and Cu/phenol/ $H_2O_2 = 1/1950/3900$ at 60 °C.

Table 2. Summary of hydroxylation reaction using Cu-SCPNs at various conditions

Entry a	Catalysts	Cu/Phenol/H ₂ O ₂	Conversion (%)	Yield (%) ^c		Selectivity (%)				TOF
				CAT b	\mathbf{HQ}^{b}	DHB ^b	CAT b	\mathbf{HQ}^{b}	\mathbf{BQ}^{d}	(h ⁻¹)
1	No catalyst	0/3160/6320	7.6	0	0	0	0	0	-	-
2	Cu-SCPN-1 e	1/3160/3160	17.4	3.3	1.6	28.5	67.5	32.5	-	550
3	Cu-SCPN-1 e	1/3160/6320	27.6	8.1	1.4	34.6	85.1	14.9	< 0.3%	872
4	Cu-SCPN-1 e	1/3160/9480	30.0	10.7	4.9	51.4	69.5	31.5	-	948
5	Cu-SCPN-2 e	1/1950/3900	26.7	7.0	5.1	45.1	58.1	41.9	< 0.5%	520
6	Cu-SCPN-1+HC1 ^f	1/3160/6320	2.5	0	0	0	0	0	-	79
7	Cu-SCPN-1+HCl ^f	1/3160/6320	1.4	0	0	0	0	0	-	44
8	Cu-SCPN-1+ AcOH ^f	1/3160/6320	15.7	0	0	0	0	0	-	496
10	Cu-SCPN-1+ TFAf	1/3160/6320	8.2	0	0	0	0	0	-	259
11	Cu-SCPN-1+ MeI ^f	1/3160/6320	20.4	2.8	0.7	17.1	79.5	20.5	-	644
12	$Cu(NO_3)_2.3H_2O$	1/3160/6320	17.5	0.8	0.7	9.2	53.3	46.7	-	553

Note: a All reactions were performed at 60 o C for 1 h in water. b DHB = dihydroxy benzene (both 1,2- and 1,4-), CAT= catechol, HQ = hydroquinone, BQ= benzoquinone. The selectivity of DHB was calculated using the sum of produced CAT and HQ. c Yield of CAT = n_{CAT}/n_{phenol} ; Yield of HQ = n_{HQ}/n_{phenol} . The conversion of phenol and the selectivity to DHB/CAT/HQ were determined using l H NMR. d The amount of BQ was determined from HPLC-MS; c Cu-SCPN-1 and Cu-SCPN-2 were prepared using P(MMA₂₁₈-co-IHPMA₄₃) and P(MMA₂₇₃-co-IHPMA₁₃₄), respectively, as indicated from Table 1. f 20-25 equivalences of acids and MeI were used with respect to IHPMA.

The importance of polymeric secondary coordination sphere was further supported by the unfolding and/or comparison to the reaction catalyzed by free Cu²⁺. When adding acids (*i.e.* HCl, AcOH, trifluoroacetic acid (TFA)) or methyl iodide (MeI) to quarternize imidazole, the unfolding of the SCPNs occurred as aforementioned. Without the presence of polymer frameworks, the catalytic selectivity and activity of unfolded Cu-SCPNs decreased dramatically as shown in Entries 6-11, Table 2. When the reaction was catalyzed by free Cu²⁺ ions (Entry 12 in Table 2), the yield of catechol was less than 1% even with a similar conversion of Entry 2 catalyzed by Cu-SCPN-1.

To summarize, we showed the use of Cu-imidazole coordination to trigger the self-folding of imidazole-functionalized polymers and mimic the catalytic activity of tyrosinase. The Cu-imidazole complexation is validated to drive the self-folding efficiently and reversibly. We demonstrated that polymer chains imposed steric hindrance to limit the Cu-imidazole complexation, to yield unsaturated Cu sites with an average coordination

number of 3.3. Folded polymer chains acted as a secondary coordination environment and modulated the reaction selectivity, although individual Cu sites and conformational landscape cannot be fine-tuned at the current stage. The flexibility of polymeric secondary coordination environment could dynamically vary the Cu-Cu distance and enable the selective hydroxylation cooperatively by adjacent two Cu sites. A high selectivity of 80% toward 1,2-hydroxylation can be achieved with an optimized Cu loading. These metal-containing polymeric SCPNs are believed to stand as conceptually new examples to mimicking the active sites of metalloenzymes.

ASSOCIATED CONTENT

Supporting Information. Synthetic details of the linear copolymers and Cu-SCPNs, characterization of linear copolymers and Cu-SCPNs, and the evaluation of the catalytic activity of Cu-SCPNs. This material is available free of charge via the Internet at http://pubs.acs.org.

Corresponding Author

iie.he@uconn.edu (JH)

ACKNOWLEDGMENT

J.H. and AAB thank financial support from the University of Connecticut. This work was partially supported by the Green Emulsions, Micelles and Surfactants (GEMS) Center.

REFERENCES

- 1. Rehder, D. *Bioinorganic chemistry*. Oxford University Press Oxford: 2014.
- 2. Decker, H.; Tuczek, F. Trends Biochem Sci 2000, 25, 392-397.
- 3. Karlin, K. D.; Tyeklár, Z. *Bioinorganic chemistry of copper*. Springer Science & Business Media: 2012.
- 4. Solomon, E. I.; Heppner, D. E.; Johnston, E. M.; Ginsbach, J. W.; Cirera, J.; Qayyum, M.; Kieber-Emmons, M. T.; Kjaergaard, C. H.; Hadt, R. G.; Tian, L. *Chemical reviews* 2014, 114, 3659-3853.
- 5. Solomon, E. I.; Sundaram, U. M.; Machonkin, T. E. *Chem Rev* 1996, 96, 2563-2606.
- 6. Korner, A.; Pawelek, J. Science 1982, 217, 1163-1165.
- 7. Matoba, Y.; Kumagai, T.; Yamamoto, A.; Yoshitsu, H.; Sugiyama, M. $J\,Biol\,Chem\,2006,\,281,\,8981\text{-}8990.$
- 8. Solomon, E. I.; Baldwin, M. J.; Lowery, M. D. *Chemical Reviews* 1992, 92, 521-542.
- 9. Malkin, R.; Malmström, B. G. Advances in Enzymology and Related Areas of Molecular Biology, Volume 33 2006, 177-244.
- 10. Casella, L.; Monzani, E.; Gullotti, M.; Cavagnino, D.; Cerina, G.; Santagostini, L.; Ugo, R. *Inorg Chem* 1996, 35, 7516-7525.
- 11. Maumy, M.; Capdevielle, P. Journal of Molecular Catalysis A: Chemical 1996, 113, 159-166.
- 12. Chioccara, F.; Chiodini, G.; Farina, F.; Orlandi, M.; Rindone, B.; Sebastiano, R. *Journal of Molecular Catalysis A: Chemical* 1995, 97, 187-194.
- 13. Sanchez-Sanchez, A.; Arbe, A.; Colmenero, J.; Pomposo, J. A. ACS Macro Letters 2014, 3, 439-443.
- 14. Tooley, C.; Pazicni, S.; Berda, E. *Polymer Chemistry* 2015, 6, 7646-7651.
- 15. Latorre-Sánchez, A.; Pomposo, J. A. *Polymer International* 2016, 65, 855-860.
- 16. Artar, M. g.; Souren, E. R.; Terashima, T.; Meijer, E.; Palmans, A. R. *ACS Macro Letters* 2015, 4, 1099-1103.
- 17. Zhu, Z.; Xu, N.; Yu, Q.; Guo, L.; Cao, H.; Lu, X.; Cai, Y.
- Macromolecular rapid communications 2015, 36, 1521-1527.
- 18. Willenbacher, J.; Altintas, O.; Trouillet, V.; Knöfel, N.; Monteiro, M. J.; Roesky, P. W.; Barner-Kowollik, C. *Polymer Chemistry* 2015, 6, 4358-4365.
- 19. Bai, Y.; Feng, X.; Xing, H.; Xu, Y.; Kim, B. K.; Baig, N.; Zhou, T.; Gewirth, A. A.; Lu, Y.; Oldfield, E. *J Am Chem Soc* 2016, 138, 11077-11080.
- 20. Greb, L.; Mutlu, H.; Barner-Kowollik, C.; Lehn, J.-M. *Journal of the American Chemical Society* 2016, 138, 1142-1145.
- 21. Berkovich, I.; Mavila, S.; Iliashevsky, O.; Kozuch, S.; Lemcoff, N. G. *Chemical Science* 2016, 7, 1773-1778.
- 22. Wang, F.; Pu, H.; Jin, M.; Wan, D. Macromol Rapid Comm 2016, 37, 330-336.
- 23. Artar, M.; Palmans, A. R. Catalysis Inside Folded Single Macromolecules in Water. In *Effects of Nanoconfinement on Catalysis*, Springer: 2017; pp 105-123.
- 24. Thanneert, S.; Nganga, J.; Amin, A. S.; Liu, B.; Jin, L.; Angeles-Boza, A.; He, J. *ChemCatChem* 2017.
- 25. Harth, E.; Van Horn, B.; Lee, V. Y.; Germack, D. S.; Gonzales, C. P.; Miller, R. D.; Hawker, C. J. *J Am Chem Soc* 2002, 124, 8653-8660.
- 26. Beck, J. B.; Killops, K. L.; Kang, T.; Sivanandan, K.; Bayles, A.; Mackay, M. E.; Wooley, K. L.; Hawker, C. J. *Macromolecules* 2009, 42, 5629-5635.
- 27. Mes, T.; van der Weegen, R.; Palmans, A. R. A.; Meijer, E. W. *Angew Chem Int Edit* 2011, 50, 5085-5089.

- 28. He, J.; Tremblay, L.; Lacelle, S.; Zhao, Y. Soft Matter 2011, 7, 2380-2386
- 29. Li, W.; Kuo, C.-H.; Kanyo, I.; Thanneeru, S.; He, J. *Macromolecules* 2014, 47, 5932-5941.
- 30. Hanlon, A. M.; Lyon, C. K.; Berda, E. B. *Macromolecules* 2015, 49, 2-14.
- 31. Gonzalez-Burgos, M.; Latorre-Sanchez, A.; Pomposo, J. A. *Chemical Society Reviews* 2015, 44, 6122-6142.
- 32. Li, W.; Thanneeru, S.; Kanyo, I.; Liu, B.; He, J. Acs Macro Lett 2015, 4, 736-740.
- 33. Mavila, S.; Eivgi, O.; Berkovich, I.; Lemcoff, N. G. Chem Rev 2016, 116, 878-961.
- 34. Altintas, O.; Barner-Kowollik, C. Macromolecular rapid communications 2016, 37, 29-46.
- 35. Basasoro, S.; Gonzalez-Burgos, M.; Moreno, A. J.; Verso, F. L.; Arbe, A.; Colmenero, J.; Pomposo, J. A. *Macromolecular rapid communications* 2016, 37, 1060-1065.
- 36. Wong, E. H.; Qiao, G. G. Macromolecules 2015, 48, 1371-1379.
- 37. Pomposo, J. A.; Rubio-Cervilla, J.; Moreno, A. J.; Lo Verso, F.; Bacova, P.; Arbe, A.; Colmenero, J. *Macromolecules* 2017.
- 38. Stals, P. J.; Gillissen, M. A.; Paffen, T. F.; de Greef, T. F.; Lindner, P.; Meijer, E.; Palmans, A. R.; Voets, I. K. *Macromolecules* 2014, 47, 2947-2954.
- 39. Pomposo, J. A.; Perez-Baena, I.; Lo Verso, F.; Moreno, A. J.; Arbe, A.; Colmenero, J. How far are single-chain polymer nanoparticles in solution from the globular state? ACS Publications: 2014.
- 40. Suh, J. Accounts Chem Res 2003, 36, 562-570.
- 41. Wang, F.; Liang, W. J.; Jian, J. X.; Li, C. B.; Chen, B.; Tung, C. H.; Wu, L. Z. Angewandte Chemie International Edition 2013, 52, 8134-8138.
- 42. Henzler-Wildman, K.; Kern, D. Nature 2007, 450, 964-972.
- 43. Hu, S.; Cattin-Ortola, J.; Munos, J. W.; Klinman, J. P. Angew. Chem., Int. Ed. 2016, 55, 9361-9364.
- 44. Świderek, K.; Tuñón, I.; Martí, S.; Moliner, V. ACS Catalysis 2015, 5, 1172-1185.
- 45. Benaglia, M.; Alberti, A.; Giorgini, L.; Magnoni, F.; Tozzi, S. *Polymer Chemistry* 2013, 4, 124-132.
- 46. Xu, F.; Chai, M.; Li, W.; Ping, Y.; Tang, G.; Yang, W.; Ma, J.; Liu, F. *Biomacromolecules* 2010, 11, 1437-1442.
- 47. Gao, H.; Lu, X.; Ma, Y.; Yang, Y.; Li, J.; Wu, G.; Wang, Y.; Fan, Y.; Ma, J. Soft Matter 2011, 7, 9239-9247.
- 48. Li, C.; Yang, Y.-W.; Liang, Z.-x.; Wu, G.-l.; Gao, H. Polym Chem-Uk 2013, 4, 4366-4374.
- 49. Zhang, G.; Wang, Y.; Liu, G. Polym Chem-Uk 2016, 7, 6645-6654.
- 50. Tuten, B. T.; Chao, D.; Lyon, C. K.; Berda, E. B. *Polym Chem-Uk* 2012, 3, 3068-3071.
- 51. Rubinstein, M.; Colby, R. H. *Polymer physics*. Oxford University Press: Oxford; New York, 2003; p xi, 440 p.
- 52. Lowe, A. B.; Billingham, N. C.; Armes, S. P. *Macromolecules* 1999, 32, 2141-2148.
- 53. Terashima, T.; Sugita, T.; Fukae, K.; Sawamoto, M. Macromolecules 2014, 47, 589-600.
- 54. Sreenivasulu, B.; Vetrichelvan, M.; Zhao, F.; Gao, S.; Vittal, J. J. Eur J Inorg Chem 2005, 2005, 4635-4645.
- 55. Zhu, Z.; Xu, N.; Yu, Q.; Guo, L.; Cao, H.; Lu, X.; Cai, Y. *Macromol Rapid Commun* 2015, 36, 1521-7.
- 56. Zhao, M.; Sun, L.; Crooks, R. M. *Journal of the American Chemical Society* 1998, 120, 4877-4878.
- 57. Van Holde, K. E.; Johnson, W. C.; Ho, P. S. 2006.
- 58. Karakhanov, E. A.; Maximov, A. L.; Kardasheva, Y. S.; Skorkin, V.
- A.; Kardashev, S. V.; Ivanova, E. A.; Lurie-Luke, E.; Seeley, J. A.; Cron, S. L. *Ind Eng Chem Res* 2010, 49, 4607-4613.
- 59. Rolff, M.; Schottenheim, J.; Decker, H.; Tuczek, F. *Chem Soc Rev* 2011, 40, 4077-4098.
- 60. Lykourinou, V.; Ming, L. J. Eur J Inorg Chem 2015, 2015, 375-381.

Table of Contents

